

Turbocharged Diesel Engine Power Production Enhancement: Proposing a Novel Thermal-Driven Supercharging System based on Kalina Cycle

F. Salek¹, A. Eskandary Nasrabad¹ and M.M. Naserian^{*1}

1- Department of Mechanical Engineering, Faculty of Montazeri, Khorasan Razavi Branch, Technical and Vocational University (TVU), Mashhad, Iran.

Receive Date 3 April 2020; Revised 26 April 2020; Accepted Date 25 May 2020

*Corresponding authors: mm.naserian@gmail.com (M. M. Naserian)

Abstract

In this paper, a novel thermal-driven supercharging system is proposed for downsizing of a turbocharged diesel engine. Furthermore, the Kalina cycle is used as a waste heat recovery system to run the mounted supercharging system. The waste heat of air in engine exhaust and intake pipes is converted to the cooling and mechanical power by the Kalina cycle. The mechanical power produced by the Kalina cycle is transferred to an air compressor to charge extra air to the engine in order to generate more power. This feature can be used for downsizing the turbo-charged heavy duty diesel engine. In addition, the heat rejected from the engine intercooler is transferred to the Kalina cycle vapor generator component, and part of the engine exhaust waste heat is also used for superheating the Kalina working fluid before entering the engine. Then the first and second law analyses are performed to assess the operation of the engine in different conditions. Moreover, an economic model is provided for the Kalina cycle, which is added to the engine as a supplementary component. Finally, the simple payback and net present value methods are used for the economic evaluation of the added supplementary system. According to the results obtained, mounting the novel waste heat-driven air charging system results in the incrementation of air mass flow rate, which leads to an extra power generation (between 9 kW and 25 kW). The payback period and the profitability index of the project are approximately 3.81 years and 1.26, respectively.

Keywords: Waste heat recovery, Diesel engine, Kalina cycle, Power production, Cooling power.

1. Introduction

Nowadays, the researchers are looking for ways to decrease fuel consumption in the internal combustion engines. One of the most efficient ways to achieve this purpose is to use the waste heat recovery (WHR) systems. The thermodynamic cycles such as the Rankine cycles [1-3], Brayton cycle [4, 5], and refrigeration cycles [6, 7] are used to recover the engine waste heat to other usable types of energy such as mechanical, electrical, and cooling energy. In some research works, the thermo-economic analysis of different types of multi-generation systems that contain various waste heat recovery systems has been performed for evaluation of their performance [8-10].

The recovered power is utilized in many ways. For instance, in the turbo-compounding systems [11-14], the power generated by the WHR systems is transferred to the engine driveline. Therefore, it is

used to increase the vehicle driving force. Recently, some other researchers have focused on using the recovered energy to run other auxiliary equipment such as air charging systems [11, 12], which result in increasing the engine thermal efficiency and the output power.

There are some researchers who have studied engine waste heat recovery by employing the Rankine cycle and transfer generated power to the engine supercharging system [15, 16]. Alessandro Romagnoli *et al.* [15] have investigated the benefits of coupling an organic Rankine cycle, which absorbs heat from engine exhaust to engine supercharger. During their research work, it was found that the implement of this technology on vehicles would decrease the engine BSFC by approximately 5%. However, other thermodynamic cycles such as the Brayton and Kalina cycles, which are widely used as WHR

systems [17], have not been examined yet as a source of power for the mentioned air supercharging system.

In this work, a novel waste heat driven supercharging system was analyzed using the thermo-economic and exergy analysis method. The Kalina cycle was employed to generate power from engine waste heat to energize the engine air charging system. The waste heat of air going through the engine intercooler and exhaust is transferred to the Kalina cycle and is converted to the cooling and mechanical power. The mechanical power is used to run a supercharger, which is mounted before air compressor in engine intake line. Thus the Kalina cycle working fluid absorbs air heat at engine intercooler, which results in reducing the air temperature. Therefore, extra air would be inhaled by the engine. The produced cooling power can be used for vehicle air conditioning system or produce cold water.

2. System description

The provided system consists of three components: air charging system, engine, and exhaust system and Kalina cycle. The air charging system contains two air compressors (Comp1 and Comp2) and a heat exchanger (HEX1) that decreases the temperature of air. In fact, some of the engine inlet air heat is absorbed by HEX1 and transferred to the Kalina cycle. Therefore, by employment of HEX1, two achievements can be made: cooling down air temperature leading to inhaling extra air by engine, and transferring air heat to the WHR system. Comp2 and Turb1 are coupled to each other as the main components of the engine turbocharging system. Turb2 is a steam turbine that is rotated by

the Kalina cycle working fluid. The output power of Turb2 is transferred mechanically to Comp1, which acts as a supercharger in the air charging system. It leads to more power and less soot productions [18, 19].

It can be figured out from figure 2 that two heat exchangers (HEX2 and HEX3) are mounted in the engine exhaust system. HEX2 is used to produce hot water for domestic or other activities. However, it does not absorb all the available heat in flue gases, so HEX3 is employed to transfer the available heat to the Kalina cycle for superheating ammonia.

As mentioned earlier, the Kalina cycle absorbs heat from two sources: engine air charging system and exhaust system. Then the waste heat is converted to the cooling and mechanical power, which is used to drive a supercharger. The cooling power can be used to produce cold water for domestic use or for air conditioning systems.

The technical specifics of the mentioned turbocharged diesel engine are provided in table 1.

Table 1. Specifications of the proposed turbocharged diesel engine [20].

Parameter	Unit	Value
Manufacturer	-	John Deere
Engine model	-	6068TF250
Engine type	-	4Cycle, Turbocharged
Cylinder arrangement	-	6 Inline
Displacement Volume	L	6.79
Bore	mm	106
Stroke	mm	127
Compression ratio		17
Rated RPM	rpm	1800
Maximum power at rated RPM	kW	142

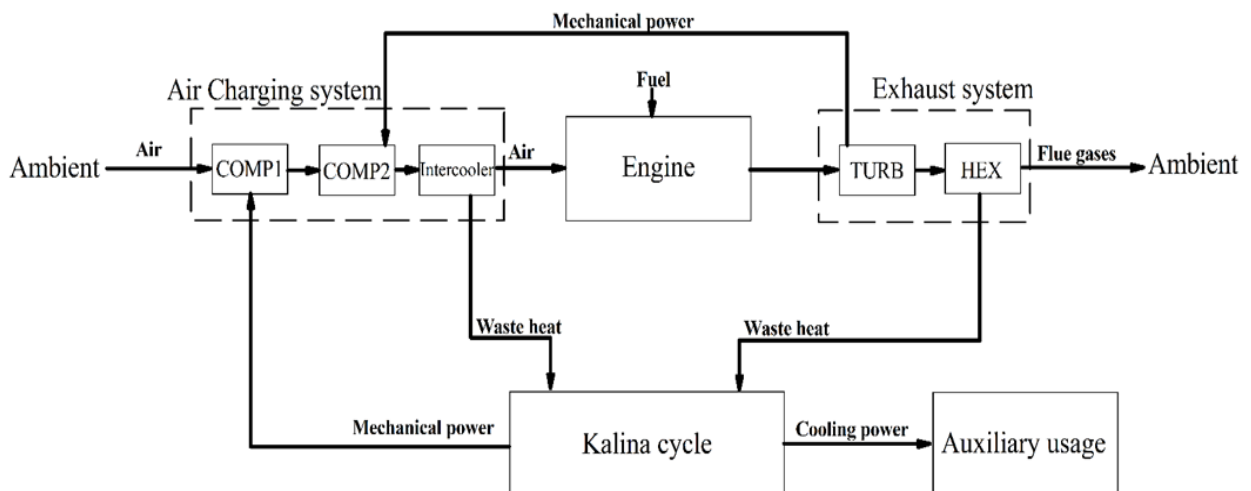


Figure 1. Energy flow diagram of system.

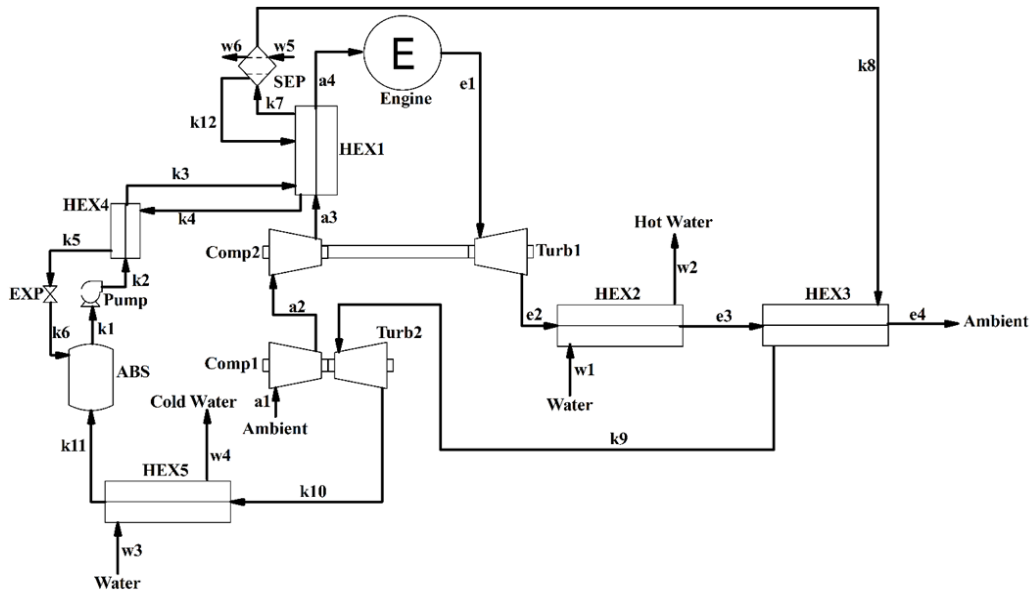


Figure 2. A block diagram of the whole system

3. Mathematical modeling

3.1. Energy modeling

Due to providing the first law analysis system, mass conservation, concentration, and energy balance equations are applied to each component of the system, which are considered as control volume [21-23].

- mass conservation:

$$\sum \dot{m}_i = \sum \dot{m}_e \quad (1)$$

- energy equation:

$$\sum \dot{Q} + \sum \dot{W} = \sum \dot{m}_e h_e - \sum \dot{m}_i h_i \quad (2)$$

- concentration equation:

$$\sum \dot{m}_i X_i = \sum \dot{m}_e X_e \quad (3)$$

Some assumptions are considered to simplify the equations:

- Each component is considered as a control volume that can exchange work and heat with ambient
- Thermodynamic equilibrium is applied to the whole system components
- Steady conditions are assumed in all points of system
- The pressure drop due to friction caused by the fluid flow inside the components is denied

3.1.1. Diesel engine

A turbocharged diesel engine includes two external and four internal thermodynamic processes. Applying the first law of thermodynamic for each process of engine [24-26]:

3.1.1.1. Air charging system

Air compressors in the air-charging system:

$$\dot{W}_{comp} = \dot{m}_a (h_e - h_i) \quad (4)$$

$$\eta_{ise.comp} = \frac{h_{ise.e} - h_i}{h_e - h_i} \quad (5)$$

Intercooler in the air-charging system:

$$\dot{Q}_{HEX1} = \dot{m}_a (h_i - h_e) \quad (6)$$

3.1.1.2. Engine internal processes

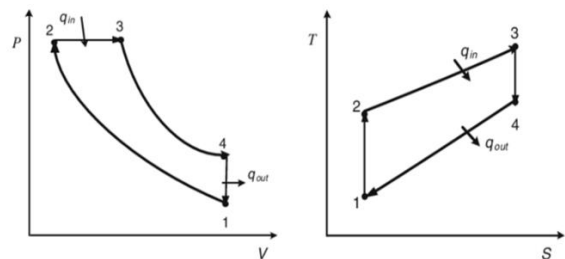


Figure 3. The T-S and P-V diagrams of the diesel cycle.

Engine intake process:

$$AF = \frac{m_a}{m_f} \quad (7)$$

$$\dot{m} = \frac{m \times N \times n_c}{2 \times 60} \quad (8)$$

$$T_1 = T_{a4} \quad (9)$$

$$P_1 = P_{a4} \quad (10)$$

$$m_{total} = m_a + m_f \quad (11)$$

$$m_{total.max} = \frac{V_{BDC}}{v_1} \quad (12)$$

$$m_{total} \leq 0.9 m_{total.max} \quad (13)$$

Engine compression process:

$$W_{cp} = m_{total}(u_2 - u_1) \quad (14)$$

$$\eta_{ise.cp} = \frac{u_{ise.2} - u_1}{u_2 - u_1} \quad (15)$$

$$r_c^k = \frac{P_2}{P_1} \quad (16)$$

Engine combustion process:

Absorbing heat in a constant pressure process:

$$Q_{comb} = m_{total}(h_3 - h_2) \quad (17)$$

Expansion in a constant pressure process:

$$Q_{comb} - W_{exp1} = m_{total}(u_3 - u_2) \quad (18)$$

$$Q_{comb} = m_{total} \times LHV \times \eta_{comb} \quad (19)$$

Expansion process:

$$W_{exp2} = m_{total}(u_3 - u_4) \quad (20)$$

$$Q_{comb} = m_{total} \times LHV \times \eta_{comb} \quad (21)$$

$$\eta_{ise.ep} = \frac{u_3 - u_4}{u_3 - u_{ise.4}} \quad (22)$$

$$\frac{P_4}{P_3} = \left[\frac{v_3}{v_4} \right]^k \quad (23)$$

Exhaling process:

$$Q_{ex} = m_{total}(u_4 - u_5) \quad (24)$$

Engine thermal efficiency and total power generation:

$$\eta_{t.diesel} = \frac{W_{output}}{\dot{m}_f LHV} \quad (25)$$

$$W_{net} = W_{exp1} + W_{exp2} - W_{cp} - V_d(P_{e1} - P_{a4}) \quad (26)$$

$$\dot{W}_{output} = \frac{W_{net} \times N \times n_c \times \eta_b \times \eta_e}{2 \times 60} \quad (27)$$

$$BSFC = \frac{\dot{m}_f}{\dot{W}_{output}} \quad (28)$$

3.1.1.3. Exhaust system

Heat exchangers:

$$\eta_{HEX} = \frac{\dot{m}_c(h_e - h_i)}{\dot{m}_e(h_i - h_e)} \quad (29)$$

Turbine 1:

$$\dot{W}_{Turb1} = \dot{m}_e(h_{e1} - h_{e2}) \quad (30)$$

$$\eta_{ise.turb} = \frac{h_i - h_e}{h_i - h_{ise.e}} \quad (31)$$

$$\dot{W}_{Turb1} \times \eta_m = \dot{W}_{comp2} \quad (32)$$

3.1.2. Kalina Cycle

In the Kalina cycle, NH₃-H₂O is employed as the working fluid. Applying the first law of thermodynamic, continuum, and concentration equations for each stream of cycle [27-29]:

Generator:

$$\dot{Q}_{HEX1} = \dot{m}_{k3}h_{k3} + \dot{m}_{k12}h_{k12} - \dot{m}_{k7}h_{k7} - \dot{m}_{k4}h_{k4} \quad (33)$$

Separator:

$$\dot{Q}_{Sep} = \dot{m}_{k7}h_{k7} - \dot{m}_{k12}h_{k12} - \dot{m}_{k8}h_{k8} \quad (34)$$

Heat exchanger 3:

$$\dot{Q}_{HEX3} = \dot{m}_{k9}h_{k9} - \dot{m}_{k8}h_{k8} \quad (35)$$

Turbine 2:

$$\dot{W}_{Turb2} = \dot{m}_{k9}h_{k9} - \dot{m}_{k10}h_{k10} \quad (36)$$

$$\dot{W}_{Turb2} \times \eta_m = \dot{W}_{comp1} \quad (37)$$

Evaporator:

$$\dot{Q}_{Evap} = \dot{m}_{k10}h_{k10} - \dot{m}_{k11}h_{k11} \quad (38)$$

Absorber:

$$\dot{Q}_{Abs} = \dot{m}_{k6}h_{k6} + \dot{m}_{k11}h_{k11} - \dot{m}_{k1}h_{k1} \quad (39)$$

Pump:

$$\dot{W}_{Pump} = \dot{m}_{k1}(h_{k2} - h_{k1}) \quad (40)$$

Expansion valve B (isenthalpic):

$$h_{k6} = h_{k5} \quad (41)$$

Strong solution concentration of ammonia and weak solution concentration of water and Turbine mechanical efficiency are considered as 0.51, 0.5853 and 0.87, respectively.

3.2. Exergy modeling

To provide the second law analysis of the system, exergy destruction for each component is obtained from equations below [30-34]:

$$I = \sum \dot{m}_i e_i - \sum \dot{m}_e e_e + \sum \dot{W} + \sum \dot{E}_Q \quad (42)$$

$$\dot{E}_Q = \left(1 - \frac{T_0}{T}\right) \dot{Q} \quad (43)$$

$$e = e_{ph} + e_{ch} \quad (44)$$

$$e_{ph} = (h_e - h_i) - T_0(s_e - s_i) \quad (45)$$

The mixture chemical exergy can be calculated by:

$$e_{ch} = \left[\sum_{i=1}^n X_i e_{ch_i} + RT_0 \sum_{i=1}^n X_i \ln(X_i)\right] \quad (46)$$

The chemical exergy of fuel (C_aH_b) that is consumed by the engine can be determined by:

$$e_f = LHV \left[1.04224 + 0.011925 \frac{b}{a} - \frac{0.042}{a}\right] \quad (47)$$

Finally, the second law efficiency of the diesel engine can be calculated by:

$$\eta_{exe.diesel} = \frac{W_{output}}{\dot{m}_f e_f} \quad (48)$$

The dead state temperature and pressure for exergy analysis are 298K and 101.325 kPa, respectively.

3.3. Economic modeling

In this work, a Kalina cycle is added to a CHP system to run a supercharger. Therefore, only the capital cost of the added cycle is considered in economic analysis. At first, the capital cost of the Kalina cycle system is calculated. Then the simple payback and net present value (NPV) methods are employed to perform the economic analysis.

The extra cost of profit per year by adding the Kalina cycle to the system can be calculated as follows:

$$Z_{ep} = \Delta \dot{W}_{output} \times Hr \times C_e - \Delta \dot{V}_f \times Hr \times C_f \quad (49)$$

where C_e and C_f are the electric power cost and fuel cost in Iran, which are considered 0.03 \$(kWh)⁻¹ and 0.09 \$ Lit⁻¹, respectively [35].

3.3.1. Capital cost

The cost of each component of the Kalina cycle is evaluated separately to obtain the capital cost of the added features. The cost of the valves and pump are not considered in calculations. In order to estimate the capital cost of the Kalina cycle, the general equation is presented as below [36]:

$$Z_{CC} = C_{0p} [B_1 + (B_2 F_m F_p)] \quad (50)$$

$$C_{0p} = 10^{(K_1 + K_2 \log(char) + K_3 (\log(char))^2)} \quad (51)$$

The char is the key parameter of each component; total volume of separator, total heat transfer area in evaporator, recuperator and condenser, and net produced power in turbine. Using the LMTD method, the total heat transfer area for heat exchangers can be calculated as:

$$\Delta T_{LMTD} = \frac{\Delta T_A - \Delta T_B}{\log \frac{\Delta T_A}{\Delta T_B}} \quad (52)$$

$$Q = UA \Delta T_{LMTD} \quad (53)$$

The rates of heat transfer as U values and the constant parameters in equation (51) are presented in tables 2 and 3, respectively. The air compressor price (Comp1) is obtained from a reference [37] and considered as 1000 dollars.

Table 2. Rates of heat transfer values for simulation [36].

Component	U (W(m ² K) ⁻¹)
Evaporator	900
Economizer	1000
Condenser	1100

3.3.2. Payback period

The simple payback period can be estimated as follows [38]:

$$pb = \frac{Z_{Invest}}{Z_{ep}} \quad (54)$$

Z_{Invest} is the total cost of components in the Kalina cycle.

3.3.3. NPV method

The net present value (NPV) method [38] is used to provide the real profitability index of the project.

$$NPV = -Z_{Invest}IF_{n=0}RDF_{n=0} + \sum_{n=1}^n Z_{ep}IF_nRDF_n \quad (55)$$

where IF and RDF are the inflation factor and the real discount factor, respectively, which are obtained from:

$$IF = \left(1 + \frac{R}{100}\right)^{-n} \quad (56)$$

$$RDF = \left(1 + \frac{RIR}{100}\right)^{-n} \quad (57)$$

$$RIR = DR - R \quad (58)$$

DR , R , and RIR are the discount rate, rate of inflation, and real interest rate, respectively. According to the reports, the inflation rate in Iran was approximately 18.4 in 2019 [39]. In addition, it is assumed that the system will work for 20 years. The profitability index (PI) can be expressed as:

$$PI = \frac{NPV + Z_{Invest}}{Z_{Invest}} \quad (59)$$

Table 3. Equations (49) and (50) constant parameters [36].

Component	K_1	K_2	K_3	B_1	B_2	F_m	F_p
Evaporator	2.7652	0.7282	0.0783	1.74	1.55	2.8	1
Recuperator	2.7652	0.7282	0.0783	1.74	1.55	2.8	1
Condenser	2.7652	0.7282	0.0783	1.74	1.55	2.8	1
Turbine	3.4092	-0.5104	0.0030	0	1	3.6	1

4. Validation

For validation of the provided mathematical model, the output data in a specific condition, the same as reference [20], is compared with each other. The data presented in table 1 is used as the input parameters of the engine model. Then the power output of the diesel engine in different loads is calculated and compared with the reference. Figure 4 indicates the engine power output in various engine loads obtained by the model and the reference. It can be easily inferred from this figure that the error percentage of the written model is below 10%.

For validation of the Kalina cycle mathematical model, the components of heat transfer rates in the written mathematical model and reference [27] are compared with each other (table 5). According to the results tabulated in table 4, the maximum error is approximately 6.27%, which is below 10%.

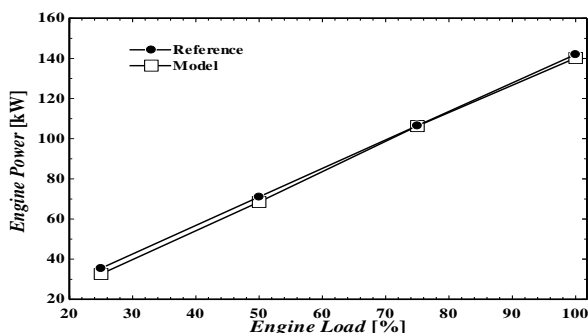


Figure 4. Engine power output in various loads in the written model and the reference [20].

Table 4. Comparison of diesel engine parameters in the catalogue [20] and the mathematical model.

Parameter	Catalogue	Model	Error [%]
Maximum power at 1800 (rated) RPM [kW]	142	142.1	0.07
Heat rejected to cooling water at rated engine power [kW]	76.3	78.5	2.8
Fuel consumption of engine at rated engine power at 100% load [L h ⁻¹]	35.6	36.61	2.76

Table 5. Comparison between the Kalina cycle components of heat transfer rates of models [27].

Parameter	Value in reference [kW]	Value in MATLAB [kW]	Error [%]
$\dot{Q}_{Generator}$	390.4	390.8	0.1
$\dot{Q}_{Evaporator}$	25.9	25.9	0
$\dot{Q}_{Separator}$	83.8	83.51	0.34
$\dot{Q}_{Absorber}$	358.8	382.8	6.27
$\dot{W}_{Turbine}$	76	76.88	1.14

5. Results and discussion

The mathematical model of the system is written in the MATLAB software to perform a mathematical analysis under specific conditions. In order to solve

the provided mathematical model, an iterative solving method based on a strategy or an algorithm is required. Thus the main algorithm for running the model is presented in figure 5.

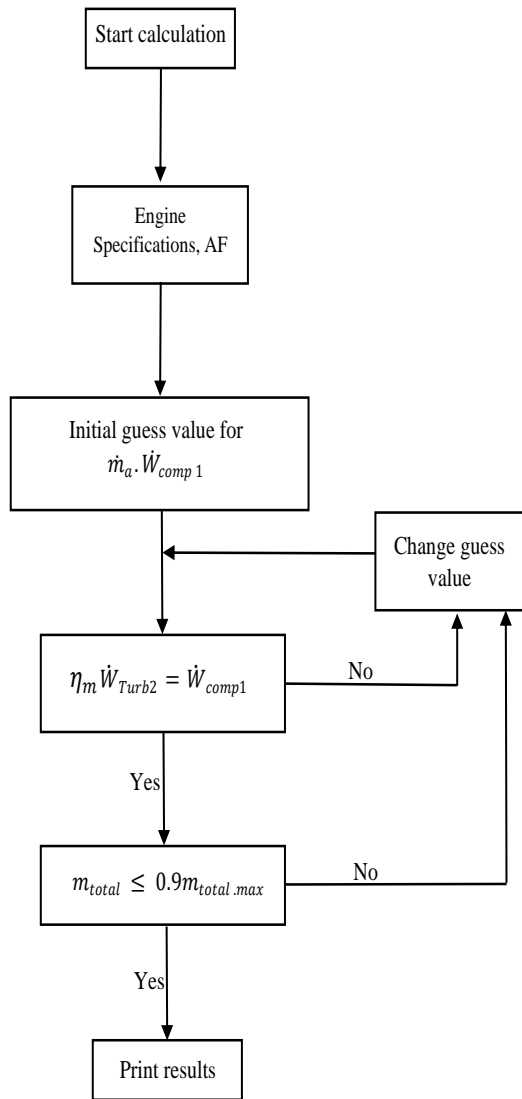


Figure 5. Mathematical iterative algorithm for solving the mathematical model of system.

The mentioned figure consists of a block diagram that shows the way of solving the whole model. As it can be seen in figure 5, after setting the initial guesses, the value of heat transferred by HEX1 would be calculated. Following that, the amount of power generated by the Kalina cycle will be found. Then the amount of generated power for Comp1 would be corrected in the solving process to find the best fitted value. Moreover, the effects of supercharging equipment on the mass of air in the engine inhaling process have to be checked. If it would be ok, the results would be generated at the final section of solving process.

Figure 6 shows the rate of power consumption (or Kalina cycle power production) when different rates of heat are absorbed by HEX1. It can be clearly seen in the figure 6 that increase in the HEX1 heat load leads to the Kalina cycle power generation increment; therefore, Comp1 power would be increased and extra air would be inhaled by the engine. As mentioned earlier, HEX1 acts as an intercooler in the engine air charging system. It decreases the air temperature at the inlet of engine so the density of air will increase. Due to the density increment of air, more air can be pushed by Comp1 and Comp2 to the engine. In addition, decrease in the air temperature at the inlet of engine can cause some other positive effects like decreasing the rate of NOx formation. The effects of employing the presented air charging system on the mass flow rate of air in engine intake manifolds can be seen in figure 7. Due to increase in the Comp1 power up to approximately 1.8 kW, the air mass flow rate is raised between 221 g/s and 244 g/s, while the air fuel ratio is constant. Hence, the rate of fuel injection would increase and more fuel can be burned in the engine, which results in producing more power.

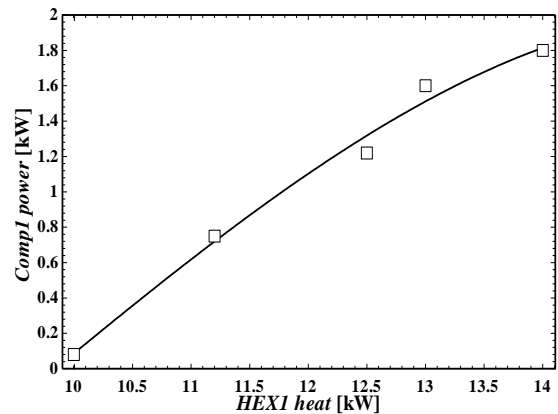


Figure 6. Comp1 power consumption in various HEX1 heat loads.

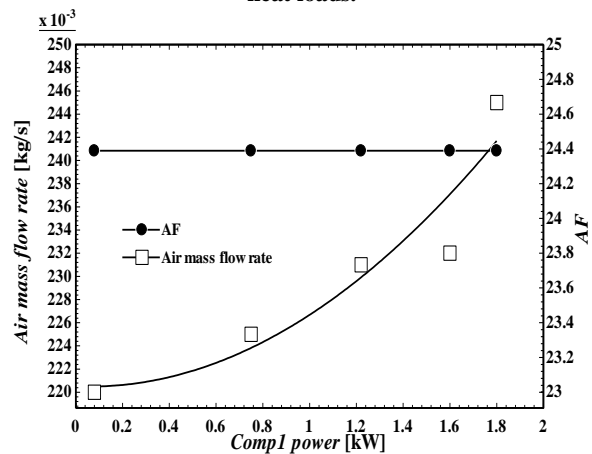


Figure 7. Air mass flow rate and air fuel ratio in various HEX1 heat loads.

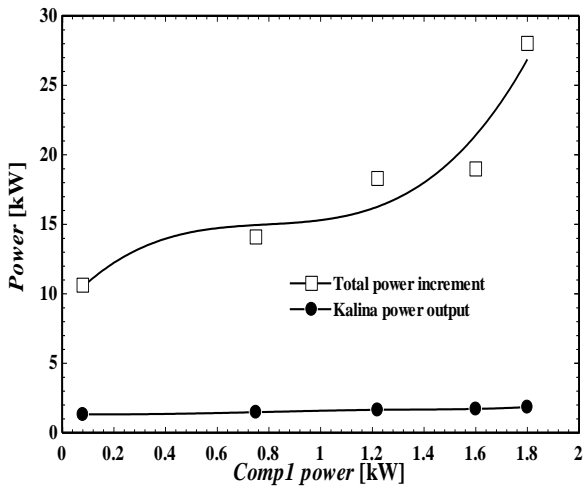


Figure 8. Engine total power increment and Kalina power output in various Comp1 powers.

The rate of power production by the Kalina cycle and engine in different Comp1 powers is presented in figure 8. It can be obviously figured out from the presented diagram that employing the Kalina power output in the engine air charging system is far more beneficial than consuming it purely. Moreover, between 9 kW and 25 kW, more power would be generated by the engine by employing the Kalina cycle power output and vapor generation system (HEX1 heat load) in the engine air charging system.

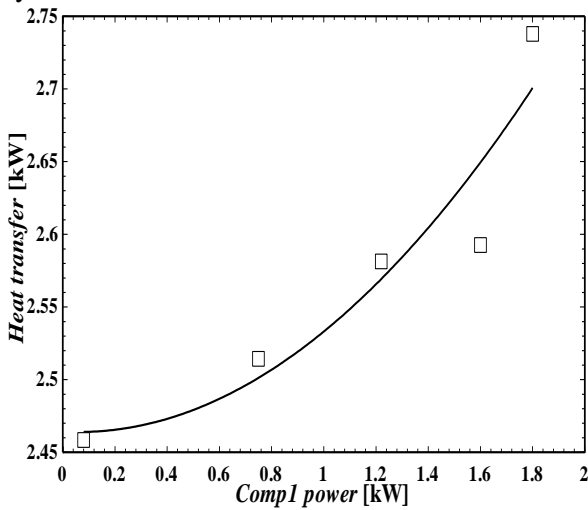


Figure 9. Rates of heat transfer for heat exchanger 3 in different Comp1 powers.

The heat exchanger 3 heat loads in various comp1 powers are presented in figure 9. In addition, this heat exchanger is used to superheat the Kalina cycle working fluid to the desired temperature. By referring to figure 9, it can be seen that up to about 2.75 kW power is absorbed by the Kalina cycle from the engine exhaust gases.

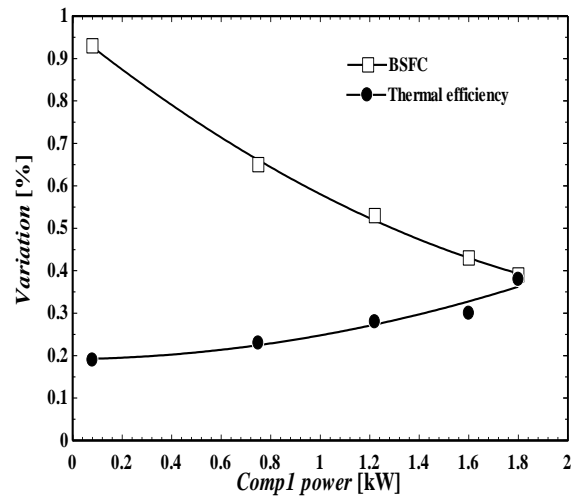


Figure 10. Variations in engine BSFC and thermal efficiency by employing the Kalina cycle in different comp1 powers.

Employment of the Kalina cycle in the engine air charging system affects the engine parameters such as BSFC and thermal efficiency, as it can be seen in figure 10. Furthermore, it decreases the engine BSFC minimally between 0.4 to approximately 1%, while increases the engine thermal efficiency up to 0.4%. Accordingly, employment of the mentioned novel air charging system does not significantly affect the engine BSFC and thermal efficiency.

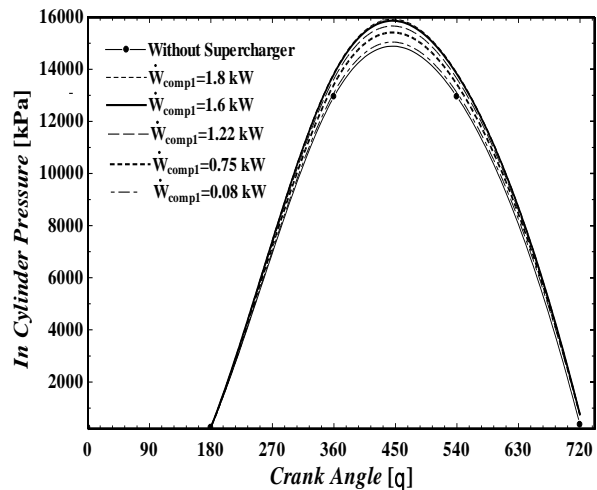


Figure 11. In cylinder pressure in different crank angles for various Comp1 power rates.

The variation in the cylinder pressure in different crank angles by employment of the air-charging system is demonstrated in figure 11. One can deduce from the figure that when a maximum power consumption of Comp1 is applied to the system, the pressure of the gas mixture in cylinders increases by 7%.

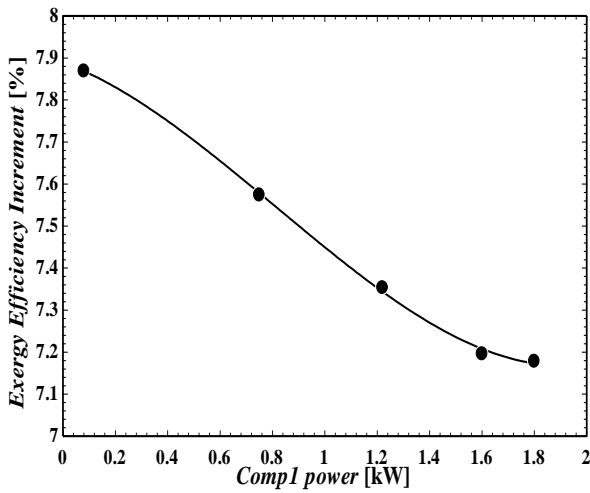


Figure 12. Total exergy efficiency increment of the system in various power consumption rates of Comp1.

By performing an exergy analysis of the system, the overall exergy efficiency of the system is obtained (figure 12). This diagram shows that due to increase in the Comp1 input power, the total exergy efficiency of the system decreases. It can be illustrated that as more fuel is injected to the engine, more power is generated, which means that more waste power is produced simultaneously. Moreover, the in cylinder pressure increment results in increase in the air temperature, which leads to more exergy destruction.

Table 6. Amounts of exergy destruction for different main components of the system with and without using the novel air charging system

Parameter	Engine exergy destruction [kW]	Bottoming cycle exergy destruction [kW]	Total exergy destruction [kW]
No supercharger	226.2	-	226.2
$\dot{W} = 1.8$ kW	250.3	3.728	254.028
$\dot{W} = 1.6$ kW	237	3.49	240.49
$\dot{W} = 1.22$ kW	235.8	3.406	239.206
$\dot{W} = 0.75$ kW	229.3	3.167	232.467
$\dot{W} = 0.08$ kW	223.8	2.95	226.75

The total exergy destruction of the system in different conditions is provided in table 6. As it can be seen in this table, with increase in the Comp1 power consumption rate, the engine exergy destruction and the total exergy destruction of the whole system are raised. In addition, the exergy destruction of the system without an air charging system (or supercharger) is lower than when it is

equipped with an air charging system because less fuel is injected to the engine.

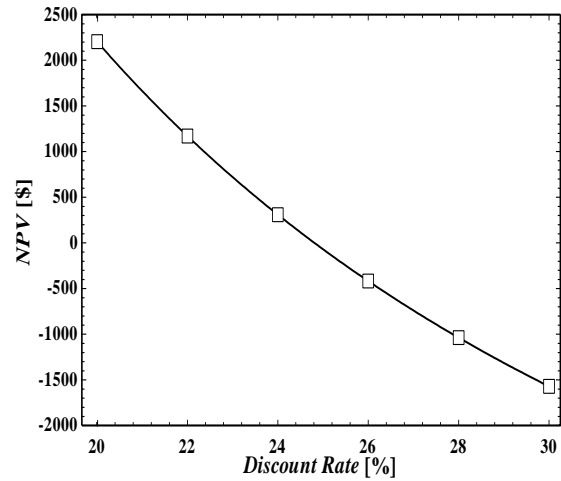


Figure 13. NPV of the project in various discount factors.

One of the main factors in the economic analysis of an energy system is the internal rate of return for the project. NPV of the project in various discount factors is presented in figure 13. The internal rate of return for the project is nearly 24.8%, which means that if the percentage of discount rate exceeds 24.8%, the project is no longer profitable. The economic assessment of adding the Kalina cycle to the diesel engine to run an air charging system is done by indicating the profitability index and payback period in different discount rates in figure 14. According to a simple payback analysis, the payback period of adding such air charging system to the engine would be approximately 3.81 years. Moreover, the profitability index is between 1.26 and 1 when the discount rate percentage changes from 20% to 24.8%. Therefore, a lesser discount rate would provide a higher profitability for the project.

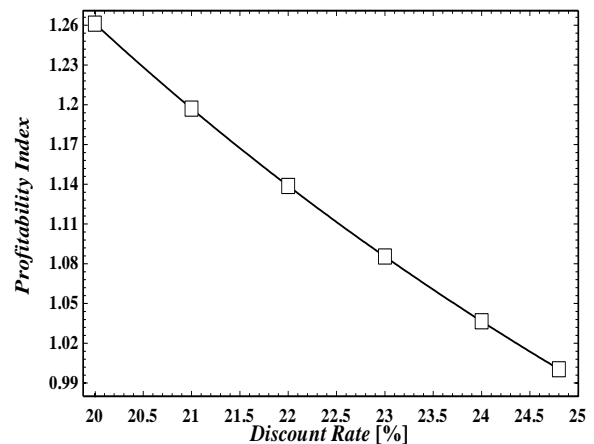


Figure 14. Profitability index and payback period of the project in various discount rates.

6. Conclusion

In this work, a novel thermal-driven supercharging system for a turbocharged diesel engine was designed and presented. In addition, some of the engine waste heat through intercooler and exhaust system was transferred to the Kalina cycle for production of the mechanical and cooling power. The produced mechanical power was used to run an air compressor, which was mounted before engine turbo-compressor for charging extra air to it. Moreover, the Kalina cycle vapor generator component, which was mounted after the engine turbo-compressor that absorbed air heat leading to reduction of air temperature, it worked as an intercooler for the mentioned turbo-charged engine. The energy and exergy analysis of the whole system was provided to evaluate the effects of different parameters on the engine performance by adding such an air charging system. Furthermore, the economic assessment of adding such an air charging system was performed by adding the Kalina cycle to a turbocharged engine. The payback period and profitability index of the proposed feature were calculated using the simple payback and NPV method. Some conclusions drawn from the analysis can be listed as follow:

- By increasing the power applied to Comp1 (up to 1.8 kW), the air mass flow rate would increase between 221 g s^{-1} and 244 g s^{-1} , while the air fuel ratio is constant.
- From 9 kW to 25 kW extra power would be generated by using the Kalina cycle and vapor generation system (HEX1 heat load) in the engine air charging system.
- Employment of the Kalina cycle in the air charging system decreases the engine BSFC minimally between 0.4% to approximately 1% and increases the engine thermal efficiency up to 0.4%.
- By transferring 1.8 kW power to Comp1, the pressure of gas mixture in the engine cylinders increase by 7%. This leads to a more engine power and a less soot production.
- The internal rate of return for the project is approximately 24.8%; therefore, the project is not profitable for discount rates higher than 24.8%.
- The payback period and profitability index of purchasing an air charging system for the engine would be approximately 3.81 years and between 1 and 1.26, respectively.

7. Acknowledgment

This project was supported by the Technical and Vocational University research support program.

Nomenclature

<i>ABS</i>	Absorber
<i>BSFC</i>	Brake specific fuel consumption [gr kWh ⁻¹]
<i>HEX</i>	Heat exchanger
<i>Comp</i>	Compressor
<i>WHR</i>	Waste heat recovery
<i>Turb</i>	Turbine
\dot{m}	Mass flow rate [kg s ⁻¹]
\dot{W}	Mechanical power [kW]
\dot{Q}	Heat power [kW]
<i>X</i>	Concentration
<i>h</i>	Enthalpy [kJ kg ⁻¹]
<i>AF</i>	Air to fuel ratio
<i>ICE</i>	Internal combustion engine
<i>N</i>	Engine RPM
<i>n</i>	Number of cylinders
<i>BDC</i>	Bottom dead center
<i>LHV</i>	Lower heating value [kJ kg ⁻¹]
<i>v</i>	Specific volume [m ³ kg ⁻¹]
<i>u</i>	Internal energy [kJ kg ⁻¹]
η	Overall efficiency
<i>P</i>	Pressure [bar]
<i>T</i>	Temperature [K] & [°C]
<i>s</i>	Entropy [kJ(kg °C) ⁻¹]
<i>r</i>	Compression ratio
<i>k</i>	Atomic coefficient
<i>Hr</i>	Hours
<i>e</i>	Exergy [kJ kg ⁻¹]
<i>C</i>	Cost
<i>Pb</i>	Payback period [years]
<i>NPV</i>	Net present value [\$]
<i>IF</i>	Inflation factor
<i>RDF</i>	Real discount factor
<i>DR</i>	Discount rate
<i>R</i>	Rate of inflation
<i>RIR</i>	Real interest rate
<i>PI</i>	Profitability index

Subscripts

<i>f</i>	Fuel
<i>i</i>	Inlet
<i>e</i>	Outlet
<i>ise</i>	Isentropic
<i>a</i>	Air
<i>cp</i>	Compressor
<i>comb</i>	Combustion
<i>exp</i>	Expansion
<i>c</i>	Compression
<i>ph</i>	Physical
<i>ch</i>	Chemical
<i>ep</i>	Electrical power
<i>cc</i>	Capital cost

References

- [1] Hoang AT. Waste heat recovery from diesel engines based on Organic Rankine Cycle. *Applied energy*. 2018;231:138-66.
- [2] Shu G, Li X, Tian H, Liang X, Wei H, Wang X. Alkanes as working fluids for high-temperature exhaust heat recovery of diesel engine using organic Rankine cycle. *Applied Energy*. 2014;119:204-17.
- [3] Xu B, Rathod D, Yebi A, Filipi Z, Onori S, Hoffman M. A comprehensive review of organic rankine cycle waste heat recovery systems in heavy-duty diesel engine applications. *Renewable and Sustainable Energy Reviews*. 2019;107:145-70.
- [4] Galindo J, Guardiola C, Dolz V, Kleut P. Further analysis of a compression-expansion machine for a Brayton Waste Heat Recovery cycle on an IC engine. *Applied Thermal Engineering*. 2018;128:345-56.
- [5] Liang Y, Bian X, Qian W, Pan M, Ban Z, Yu Z. Theoretical analysis of a regenerative supercritical carbon dioxide Brayton cycle/organic Rankine cycle dual loop for waste heat recovery of a diesel/natural gas dual-fuel engine. *Energy Conversion and Management*. 2019;197:111845.
- [6] Liang Y, Shu G, Tian H, Sun Z. Investigation of a cascade waste heat recovery system based on coupling of steam Rankine cycle and NH₃-H₂O absorption refrigeration cycle. *Energy conversion and management*. 2018;166:697-703.
- [7] Zoghi M, Habibi H, Chitsaz A, Javaherdeh K, Ayazpour M. Exergoeconomic analysis of a novel trigeneration system based on organic quadrilateral cycle integrated with cascade absorption-compression system for waste heat recovery. *Energy Conversion and Management*. 2019;198:111818.
- [8] Ahmadi MH, Alhuyi Nazari M, Sadeghzadeh M, Pourfayaz F, Ghazvini M, Ming T, et al. Thermodynamic and economic analysis of performance evaluation of all the thermal power plants: A review. *Energy science & engineering*. 2019;7(1):30-65.
- [9] Mohammadi A, Ashouri M, Ahmadi MH, Bidi M, Sadeghzadeh M, Ming T. Thermoeconomic analysis and multiobjective optimization of a combined gas turbine, steam, and organic Rankine cycle. *Energy Science & Engineering*. 2018;6(5):506-22.
- [10] Shams Ghoreishi SM, Akbari Wakilabadi M, Bidi M, Khomeini Poorfar A, Sadeghzadeh M, Ahmadi MH, et al. Analysis, economical and technical enhancement of an organic Rankine cycle recovering waste heat from an exhaust gas stream. *Energy Science & Engineering*. 2019;7(1):230-54.
- [11] Zi D, Zhang L, Chen B, Zhang Q. Study of the electric-booster and turbo-generator system and its influence on a 1.5 L gasoline engine. *Applied Thermal Engineering*. 2019;162:114236.
- [12] Joshi S, Koehler E, Dahodwala M, Franke M, Naber JD, editors. *Controls Development and Vehicle Drive Cycle Analysis of Integrated Turbocompounding, Electrification and Supercharging System (ITES)*. ASME 2018 Internal Combustion Engine Division Fall Technical Conference; 2019: American Society of Mechanical Engineers Digital Collection.
- [13] Choi B, Jung D, Lee J. Mechanical and Electromagnetic Analysis of High Speed Motor/Generator for Electric Turbo Compounding System. *The Open Electrical & Electronic Engineering Journal*. 2018;12(1).
- [14] Naseri A, Fazlikhani M, Sadeghzadeh M, Naeimi A, Bidi M, Tabatabaei SH. Thermodynamic and Exergy Analyses of a Novel Solar-Powered CO₂ Transcritical Power Cycle with Recovery of Cryogenic LNG Using Stirling Engines. *Renewable Energy Research and Application*. 2020;1(2):175-85.
- [15] Jiménez-Arreola M, Dal Magro F, Romagnoli A, Chiong MS, Rajoo S, Martinez-Botas RF, editors. *Analytical Investigation of a Thermal-Supercharged Internal Combustion Engine Compounded With Organic Rankine Cycle for Waste Heat Recovery*. ASME Turbo Expo 2017: Turbomachinery Technical Conference and Exposition; 2017: American Society of Mechanical Engineers Digital Collection.
- [16] Mahmoudzadeh Andwari A, Pesiridis A, Esfahanian V, Salavati-Zadeh A, Karvountzis-Kontakiotis A, Muralidharan V. A comparative study of the effect of turbocompounding and ORC waste heat recovery systems on the performance of a turbocharged heavy-duty diesel engine. *Energies*. 2017;10(8):1087.
- [17] Ghorbani B, Mehrpooya M, Sadeghzadeh M. Developing a tri-generation system of power, heating, and freshwater (for an industrial town) by using solar flat plate collectors, multi-stage desalination unit, and Kalina power generation cycle. *Energy Conversion and Management*. 2018;165:113-26.
- [18] Hariram V, Shangar RV. Influence of compression ratio on combustion and performance characteristics of direct injection compression ignition engine. *Alexandria Engineering Journal*. 2015;54(4):807-14.
- [19] Agarwal AK, Srivastava DK, Dhar A, Maurya RK, Shukla PC, Singh AP. Effect of fuel injection timing and pressure on combustion, emissions and performance characteristics of a single cylinder diesel engine. *Fuel*. 2013;111:374-83.
- [20] Egan B, Dechant S, Damm C. AC 2007-1342: Building as a power plant modeling and selection of a combined heat and power system for an advanced commercial building. *age*. 2007;12:1.
- [21] Sonntag RE, Borgnakke C, Van Wylen GJ, Van Wyk S. *Fundamentals of thermodynamics*: Wiley New York; 1998.
- [22] Wang J, Yan Z, Zhou E, Dai Y. Parametric analysis and optimization of a Kalina cycle driven by solar energy. *Applied Thermal Engineering*. 2013;50(1):408-15.

- [23] Salek F, Moghaddam AN, Naserian MM. Thermodynamic analysis of diesel engine coupled with ORC and absorption refrigeration cycle. *Energy Conversion and Management*. 2017;140:240-6.
- [24] Dhamecha MTSA, Tiwari P. Thermodynamic Analysis of Organic Rankine Cycle using EES Solver. 2019.
- [25] Pulkrabek WW. Engineering fundamentals of the internal combustion engine. American Society of Mechanical Engineers Digital Collection; 2004.
- [26] Lion S, Taccani R, Vlaskos I, Scrocco P, Vouvakos X, Kaiktsis L. Thermodynamic analysis of waste heat recovery using Organic Rankine Cycle (ORC) for a two-stroke low speed marine Diesel engine in IMO Tier II and Tier III operation. *Energy*. 2019.
- [27] Xu F, Goswami DY, Bhagwat SS. A combined power/cooling cycle. *Energy*. 2000;25(3):233-46.
- [28] Zare V, Mahmoudi SS, Yari M, Amidpour M. Thermoeconomic analysis and optimization of an ammonia–water power/cooling cogeneration cycle. *Energy*. 2012;47(1):271-83.
- [29] Adewusi S, Zubair SM. Second law based thermodynamic analysis of ammonia–water absorption systems. *Energy conversion and management*. 2004;45(15-16):2355-69.
- [30] Abusoglu A, Kanoglu M. Exergetic and thermoeconomic analyses of diesel engine powered cogeneration: Part 1–Formulations. *Applied Thermal Engineering*. 2009;29(2-3):234-41.
- [31] Ghaebi H, Parikhani T, Rostamzadeh H, Farhang B. Proposal and assessment of a novel geothermal combined cooling and power cycle based on Kalina and ejector refrigeration cycles. *Applied Thermal Engineering*. 2018;130:767-81.
- [32] Rakopoulos C, Giakoumis E. Simulation and exergy analysis of transient diesel-engine operation. *Energy*. 1997;22(9):875-85.
- [33] Abusoglu A, Kanoglu M. First and second law analysis of diesel engine powered cogeneration systems. *Energy Conversion and Management*. 2008;49(8):2026-31.
- [34] Long R, Kuang Z, Li B, Liu Z, Liu W. Exergy analysis and performance optimization of Kalina cycle system 11 (KCS-11) for low grade waste heat recovery. *Energy Procedia*. 2019;158:1354-9.
- [35] Fuel Cost. Available from: <https://www.globalpetrolprices.com>.
- [36] Ashouri M, Vandani AMK, Mehrpooya M, Ahmadi MH, Abdollahpour A. Techno-economic assessment of a Kalina cycle driven by a parabolic Trough solar collector. *Energy conversion and management*. 2015;105:1328-39.
- [37] Compressor price. Available from: www.melett.com.
- [38] Beggs C. *Energy: management, supply and conservation*: Routledge; 2010.
- [39] Inflation rate. Available from: www.cbi.ir.